Impedance Design of 21-kW Quasi-Z-Source H-Bridge Module for MW-Scale Medium-Voltage Cascaded Multilevel Photovoltaic Inverter

Yushan Liu[1,2], *Student Member*, *IEEE*
[1]School of Electrical Engineering
Beijing Jiaotong University
Beijing 100044, China
Email: yushan.liu@qatar.tamu.edu

Haitham Abu-Rub[2], *Senior Member*, *IEEE*
[2]Department of Electrical and Computer Engineering
Texas A&M University at Qatar
Doha 23874, Qatar
Email: haitham.abu-rub@qatar.tamu.edu

Baoming Ge[1,3], *Member*, *IEEE*
[3]Department of Electrical Engineering
Texas A&M University
College Station, TX 77843, USA
Email: gebaoming@tsinghua.org.cn

Fang Zheng Peng[4], *Fellow*, *IEEE*
[4]Department of Electrical and Computer Engineering
Michigan State University
East Lansing, MI 48824, USA
Email: fzpeng@egr.msu.edu

***Abstract*— An impedance parameter design of quasi-Z-source (qZS) H-bridge inverter module applied to megawatt (MW)-scale medium-voltage Photovoltaic (PV) power system is proposed. A double-line-frequency (2ω) voltage and current ripple model of qZS network with PV panel is established. The effects of qZS inductance and capacitance as well as PV panel terminal capacitance on 2ω voltage and current ripples are investigated by using the built model. Elaborate designed prototype parameters are to buffer those low-frequency ripples. Simulations are carried out on a 21-kW single-phase qZS PV inverter to verify the proposed 2ω-ripple model and impedance design method.**

***Keywords*— Low-frequency ripple; photovoltaic power system; single-phase system; quasi-Z-source inverter.**

I. INTRODUCTION

Currently, the fast increase of world's power demand is motivating large-scale Photovoltaic (PV) power conversion systems stepping into the multi-megawatt (MW) range. There are already over 80 PV plants with capacity of more than 25 MW each, most of which were commissioned during 2011 and 2012 [1]. The medium-voltage (MV) power conversion technology is generally favored for MW-scale PV generation systems in terms of higher power density, reduced current level, and associated losses and costs, etc. For a high-power PV system, the inverter technology will be a big challenge. The existing high power (100 kW-to-MW) PV inverter topologies mainly include the central inverter, DC/DC converter plus inverter, dual inverter, and cascade multilevel inverter (CMI) [2]. Among them, the CMI has been identified as a suitable topology due to transformerless, modular structure, high efficiency, high power density, and low cost [3]. However, since lack of boost function, the traditional CMI will lead to overrating the inverter by a factor of two to cope with wide PV voltage variations.

Recently, quasi-Z-source cascade multilevel inverter (qZS-CMI) based PV power systems were presented to mitigate the defects of conventional CMI by embedding the quasi-Z-source (qZS) topology into CMI [4]-[10]. The quasi-Z-source inverter (qZSI) that can deal with the wide PV voltage variations and improve the inverter reliability as single-stage inverter topology has attracted increasing interests in PV applications [11]-[17]. And the qZS-CMI for PV power conversion presents promising features such as the balanced and constant dc-link peak voltage due to the buck/boost ability of qZS H-bridge inverter (qZS-HBI) module, the distributed maximum power point tracking to always capture the maximum PV power independently, and one-third module reduction compared with the conventional CMI. All of these will improve the reliability, cost, and volume of PV systems.

The inductance and capacitance parameters of qZS network are critical issue. References [12], [16], and [18] presented impedance design for three-phase qZSI, where the inductance and capacitance were used to limit the high-frequency ripples on qZS inductor current and capacitor voltage. However, the qZS-HBI exists low-frequency pulsating power, viz., double-line-frequency (2ω) ripples. Those 2ω power ripples introduce low-frequency ripples on qZS inductor currents, capacitor voltages, and also dc-link voltage, which can increase ac output harmonics. In the passive ripple reduction way, the impedance of qZS network is critical to buffer those 2ω ripples. Especially in MW MV qZS-CMI based PV systems, even though the qZS-HBI module's power can be reduced by cascading more modules per phase, there will still be tens of kilowatts in each module. References [19] and [20] proposed impedance design to limit 2ω ripples of single-phase ZSI/qZSI. However, they are only for low-power systems, less than 1 kW. On the other hand, the ideal DC sources were discussed as power source.

Whereas, the PV panel's internal resistance also affects the module's pulsating power. So far, no literature has investigated the impedance design of high-power qZS-HBI module for PV power conversions.

The novelty of this paper is to investigate the 2ω-ripple components of the qZS H-bridge PV inverter module in terms of a built small-signal model, and to present an effective impedance design for buffering those ripples in a 21-kW system. The organization of the paper is as follows: Section II analyzes the 2ω ripples of qZS-HBI PV module; the effects of impedance parameters on 2ω ripples are discussed in Section III; Section IV presents the impedance design method to limit the 2ω ripples; simulation investigations on a 21-kW system are addressed in Section V; finally, Section VI concludes this work.

II. Low-Frequency Ripples of Single-Phase Quasi-Z-Source Photovoltaic Inverter

Fig. 1 shows the qZS H-bridge inverter based PV module, which couples the qZS impedance network between the PV array and H-bridge inverter dc link. The qZS network combines two inductors L_1 and L_2, and two capacitors C_1 and C_2, and one diode D_1. A MW PV system can be fulfilled by series connection of tens of this basic module [4]-[10].

There is shoot-through and nonshoot-through two working states in the qZS-HBI module, as the equivalent circuits show in Fig. 2. Fig. 2 (a) shows that of the shoot-through state, i.e., the PV array and qZS capacitors charge the inductors and the diode is cut off due to negative voltage. There is

$$\begin{cases} v_{PV} = L_1 \dfrac{di_{L1}}{dt} - v_{C2} \\ v_{C1} = L_2 \dfrac{di_{L2}}{dt} \\ C_1 \dfrac{dv_{C1}}{dt} = -i_{L2} \\ C_2 \dfrac{dv_{C2}}{dt} = -i_{L1} \\ C_p \dfrac{dv_{PV}}{dt} = i_{PV} - i_{L1} \end{cases} \tag{1}$$

where v_{PV} represents output voltage of independent PV arrays; v_{L1}, v_{L2}, i_{L1}, and i_{L2} are voltages and currents of qZS inductors L_1 and L_2; v_{C1}, v_{C2} and i_{C1}, i_{C2} are voltages and currents of qZS capacitors C_1 and C_2, respectively; v_{diode} and i_{diode} are voltage and current of qZS diode, respectively; v_{DC} and i_{DC} are dc-link voltage and current, respectively.

Fig. 2 (b) shows equivalent circuit of the nonshoot-through state, the PV panel and qZS inductors charge the loads and capacitors, and the diode conducts. There is

$$\begin{cases} v_{PV} = L_1 \dfrac{di_{L1}}{dt} + v_{C1} \\ v_{C2} = -L_2 \dfrac{di_{L2}}{dt} \\ C_1 \dfrac{dv_{C1}}{dt} = i_{L1} - i_{DC} \\ C_2 \dfrac{dv_{C2}}{dt} = i_{L2} - i_{DC} \\ C_p \dfrac{dv_{PV}}{dt} = i_{PV} - i_{L1} \end{cases} \tag{2}$$

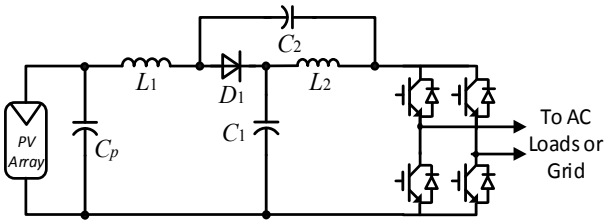

Fig. 1. Discussed qZS H-bridge inverter based PV module.

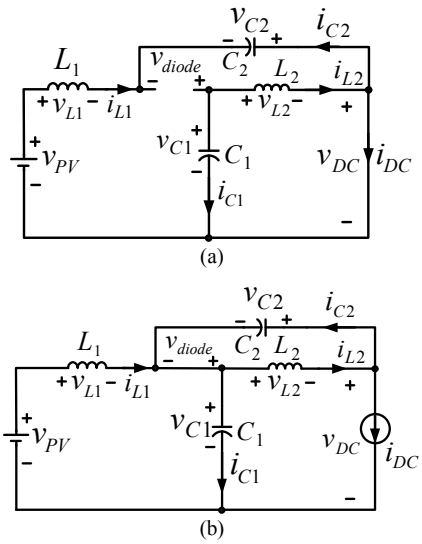

Fig. 2. Equivalent circuits of qZS-HBI in the (a) shoot-through state and (b) nonshoot-through state.

Therefore, by the small perturbance method, the ac small-signal model of qZSI can be obtained as

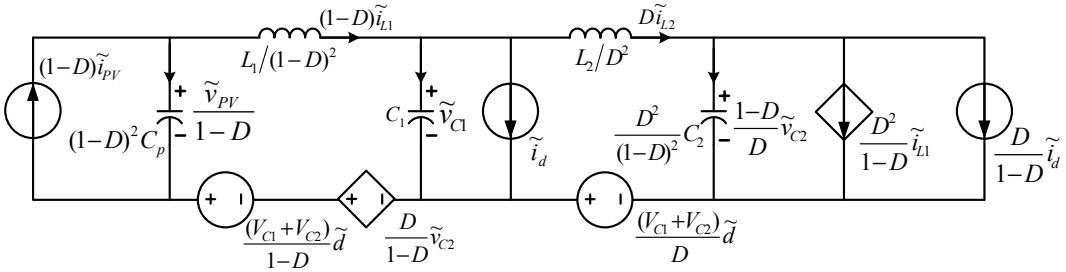

Fig. 3. AC small-signal equivalent circuit of qZSI.

$$\begin{cases} L_1\tilde{i}_{L1} = -(1-D)\tilde{v}_{C1} + D\tilde{v}_{C2} + \tilde{v}_{pv} + (V_{C1}+V_{C2})\tilde{d} \\ L_2\tilde{i}_{L2} = D\tilde{v}_{C1} - (1-D)\tilde{v}_{C2} + (V_{C1}+V_{C2})\tilde{d} \\ C_1\tilde{v}_{C1} = (1-D)\tilde{i}_{L1} - D\tilde{i}_{L2} - (1-D)\tilde{i}_{DC} - (2I_L - I_{DC})\tilde{d} \\ C_2\tilde{v}_{C2} = -D\tilde{i}_{L1} + (1-D)\tilde{i}_{L2} - (1-D)\tilde{i}_{DC} - (2I_L - I_{DC})\tilde{d} \\ C_p\tilde{v}_{pv} = \tilde{i}_{pv} - \tilde{i}_{L1} \end{cases} \quad (3)$$

where $\tilde{d}$ is the small-signal perturbance of shoot-through duty ratio; $\tilde{i}_{DC}$ is the dc-link current ripple. Assuming unit power factor for the PV system, there is

$$i_{DC} = \frac{1}{2} I_m M[1-\cos(2\omega t)] = I_{DC} + \tilde{i}_{DC} \quad (4)$$

where I_m is the magnitude of ac load current; M is the modulation index; $I_{DC} = \frac{1}{2} I_m M$ represents the dc-link current. And

$$\tilde{i}_{DC} = -\frac{1}{2} I_m M \cos(2\omega t) \quad (5)$$

represents the ripple component of dc-link current, which reveals the 2ω ripple source of the qZS-HBI module.

Based on the small-signal model of (3), the AC small-signal equivalent circuit of qZSI with PV panel terminal capacitor is obtained in Fig. 3, where $\tilde{i}_d(t)$ stands for $(1-D)\tilde{i}_{DC} + (2I_L - I_{DC})\tilde{d}$.

Moreover, the PV panel voltage has the dynamic relation with its current and internal resistance of $\tilde{v}_{PV} = -R_s\tilde{i}_{PV}$ [13]. Assuming L_1=L_2=L and C_1=C_2=C to simplify the deduction. Therefore, from (3) and Fig. 3, the 2ω-ripple components of PV voltage, inductor L_1 and L_2 currents, and capacitor C_1 and C_2 voltages can be solved, respectively.

In addition, in steady states there are

$$V_{C1} = \frac{1-D}{1-2D} V_{PV},\ V_{C2} = \frac{D}{1-2D} V_{PV},$$
$$I_{L1} = I_{L2} = I_L = \frac{P}{V_{PV}},$$
$$B = \frac{1}{1-2D},\ \hat{v}_{DC} = V_{C1} + V_{C2} = BV_{PV} \quad (6)$$

where V_{PV} is the average PV voltage; V_{C1} and V_{C2} are the average voltages of capacitor C_1 and C_2, respectively; I_{L1} and I_{L2} are the average currents of inductor L_1 and L_2, respectively; D and B are shoot-through duty ratio and boost factor of the qZSI, respectively.

III. Analysis of Impedance Parameters on 2Ω Voltage and Current Ripples

From the derived ac small-signal model and average values of (6), the peak-to-peak 2ω-ripple ratios of the variables are defined respectively

$$di_{L1} = \frac{2\hat{\tilde{i}}''_{L1}}{I_{L1}},\ di_{L2} = \frac{2\hat{\tilde{i}}''_{L2}}{I_{L2}}$$
$$dv_{PV} = \frac{2\hat{\tilde{v}}''_{PV}}{V_{PV}},\ dv_{DC} = \frac{2(\hat{\tilde{v}}''_{C1} + \hat{\tilde{v}}''_{C2})}{V_{dc}} \quad (7)$$

where di_{L1} and di_{L2} are the peak-to-peak 2ω-ripple ratios of inductor L_1 and L_2 currents, respectively; dv_{PV} is that of PV panel voltage; and dv_{DC} is that of dc-link peak voltage. The variables $\tilde{v}''_{PV}$, $\tilde{i}''_{L1}$, $\tilde{i}''_{L2}$, $\tilde{v}''_{C1}$ and $\tilde{v}''_{C2}$, with "^" stand for the magnitudes of 2ω voltage and current ripples.

Fig. 4 shows the 2ω-ripple ratios versus impedance variations. Fig. 4 (a) is the peak-to-peak 2ω-ripple ratio of PV panel voltage versus C_p and C when L is 3 mH; Fig. 4 (b) and Fig. 4 (c) are the peak-to-peak 2ω-ripple ratios of inductor currents versus C and L when C_p is 1.1 mF. Meanwhile, the average PV voltage V_{PV} is 300 V, and shoot-through duty ratio is 0.286, which achieves 702-V dc-link peak voltage.

From the peak-to-peak 2ω ripple of PV panel voltage of Fig. 4 (a), it can be seen that C_p and C are larger, the 2ω ripple of PV voltage is smaller. Comparing Fig. 4 (b) and (c), it can be concluded that the ripples of i_{L1} and i_{L2} are unequal when considering the PV internal resistance, while they are identical in [19], [20]. Even though di_{L1} is larger with C decrease, di_{L1} is still smaller than di_{L2} at the same impedance parameters. Meanwhile, C and L have combined effects on di_{L1} and di_{L2}.

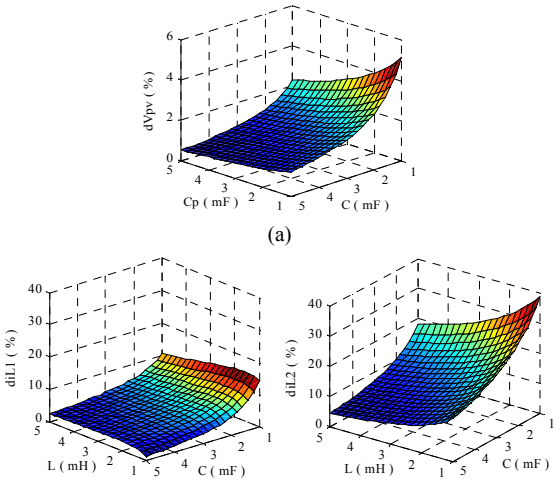

Fig. 4. Peak-to-peak 2ω-ripple ratios of (a) dv_{PV} versus C_p and C (L=3 mH); (b) di_{L1} versus L and C (C_p=1.1 mF); (c) di_{L2} versus L and C (C_p=1.1 mF).

IV. Proposed Impedance Design to Buffer 2Ω Ripples

A design example is illustrated in terms of a qZS-CMI based 1 MW-MV PV power generation system, where 16 qZS-HBI modules are cascaded per phase. In this way, each qZS-HBI module will have nearly 21-kW power. Table I lists

the detailed system operating parameters, in which HF stands for high-frequency.

TABLE I. DESIRED OPERATING PARAMETERS.

Parameters	*Values*
PV array voltage, v_{PV}	300~600 V
Power rating of qZS-CMI, P_m	1 MW
RMS phase-to-phase voltage of three-phase ac output, U_{AC}	6.6 kV
Cascaded qZS-HBI modules per phase, n	16
AC load frequency, f_0	50 Hz
Switching frequency, f_s	5 kHz
Desired HF and 2ω current ripples through the qZS inductors, di_L^*	25%
Desired 2ω ripple of PV panel voltage, dv_{PV}^*	2%
Desired 2ω ripple of dc-link peak voltage, dv_{DC}^*	6%

A. qZS Inductance

In shoot-through state, the two qZS inductors L_1 and L_2 discharge and the voltages across them equal to the capacitor-C_1 voltage v_{C1}, seen from (1). Thus to limit the high-frequency (HF) current ripple and to avoid the discontinuous conduction of inductors, from (1) and (6), the qZS inductance should be at least

$$L_{HF}=\frac{v_L\Delta T}{\Delta I_L}=\frac{V_{C1}(T_sD_{\max}/k_{sh})}{(P_{\max}/v_{PV,\min})di_L^*}=\frac{D_{\max}(1-D_{\max})v_{PV,\min}^2}{k_{sh}f_sP_m(1-2D_{\max})di_L^*} \quad (8)$$

where k_{sh} represents the shoot-through times per control period. At the worst operating case, the shoot-through duty ratio reaches its maximum, which can be solved as for simple boost control [12]

$$G_{\max}=\frac{\sqrt{2}U_{AC}}{\sqrt{3}nV_{PV,\min}},\ M_{\min}=\frac{G_{\max}}{2G_{\max}-1},\ D_{\max}=1-M_{\min} \quad (9)$$

Meanwhile, from the aforementioned analysis of 2ω ripples versus impedance parameters, when the 2ω ripple of PV panel voltage is zero, there is $\tilde{i}_{L1}''=\tilde{i}_{L2}''=\tilde{i}_L''=di_L^*I_L$. Then from (6), it can be obtained that

$$\tilde{v}_{DC}''=\tilde{v}_{C1}''+\tilde{v}_{C2}''=\frac{4\omega L}{1-2D}\tilde{i}_L''+\frac{2}{1-2D}\tilde{v}_{PV}'' \quad (10)$$

Hence, the qZS inductance for buffering 2ω ripples is at least

$$L_{2\omega}=\frac{(1-2D_{\max})dv_{DC}^*\hat{v}_{DC}}{4\omega di_L^*I_{L,\min}} \quad (11)$$

Through (8) and (11), the qZS inductance should satisfy

$$L\ge\max(L_{HF},L_{2\omega}) \quad (12)$$

B. qZS Capacitance and PV Terminal Capacitance

Two quasi-Z-source capacitors are in series in nonshoot-through states to limit the voltage ripple on the inverter bridge to dv_{DC}^* of the maximum dc-link voltage so as to keep the output voltage sinusoidal [12]. Therefore, from the derived AC equivalent model of (3), the dc-link voltage ripple is

$$\tilde{v}_{DC}=\tilde{v}_{C1}+\tilde{v}_{C2}=\frac{1-2D}{\omega C}\tilde{i}_L-\frac{1-D}{\omega C}\tilde{i}_{DC}-\frac{2I_L-I_{DC}}{\omega C}\tilde{d} \quad (13)$$

Then the qZS capacitance for buffering 2ω ripples needs to satisfy

$$C\ge\frac{(1-2D_{\max})\Delta i_{L,\max}+(1-D_{\max})\Delta i_{DC,\max}-\Delta d_{\min}(2I_L-I_{DC})}{\omega\Delta\tilde{v}_{DC}}=\frac{(1-2D_{\max})\Delta i_{L,\max}+(1-D_{\max})M_{\min}I_m}{\omega dv_{DC}^*\hat{v}_{DC}} \quad (14)$$

When the PV panel terminal capacitor is used to reduce the 2ω-ripple ratio of PV panel voltage to dv_{PV}^*, from (6), there is

$$C_p\ge\left|-\frac{a_4R_s}{2\omega a_3\tilde{v}_{PV}''}\tilde{i}_{DC}-\frac{1}{2\omega}+\frac{a_2CD_{\max}+a_1C(1-D_{\max})}{a_3}\right| \quad (15)$$

Taking into account of Fig. 4, the requirements in Table I, and (8)-(15), the 3.3 mH qZS inductance, 4.7 mF qZS capacitance, and 1.1 mF PV terminal capacitance are selected.

V. SIMULATION INVESTIGATIONS

The deduced 2ω-ripple components are investigated on a single-phase qZSI based PV system with calculated impedance parameters and system specifications in Table I. The PV panel voltage is 300 V. At the 0.7 modulation index, the 702-V dc-link peak voltage of each qZS-HBI module is required to get the 6.6-kV line voltage; hence, the shoot-through duty ratio is 0.286. From (6), the average inductor current is 70 A, capacitor C_1 voltage is 501 V, and capacitor C_2 voltage is 201 V, theoretically.

Figs. 9 and 10 show the calculated results from established 2ω-ripple model and simulated results. They are PV panel voltage v_{PV}, qZSI's dc-link voltage v_{DC}, inductor currents i_{L1} and i_{L2}, and capacitor voltages v_{C1} and v_{C2}, respectively.

As seen from Fig. 9 (a) and (b), (c) and (d), as well as Fig. 10 (a) and (b), (c) and (d), respectively, the 2ω ripples are introduced to the qZSI's dc-link voltage, qZS inductor currents, qZS capacitor voltages, and PV panel's voltage and current. It is noticeable that the theoretical calculation from the built 2ω-ripple model matches simulation very well.

By the presented parameter design method, the peak-to-peak 2ω-ripple components are limited within the desired ranges. For example, the dv_{PV} is 1.33% from Fig. 9 (a) and (b), and dv_{DC} equals to 5.7% from Fig. 9 (c) and (d); di_{L1} and di_{L2} are within 25%, seen from Fig. 10 (a) and (b). Moreover, the results of the built 2ω-ripple model match the simulation results very well.

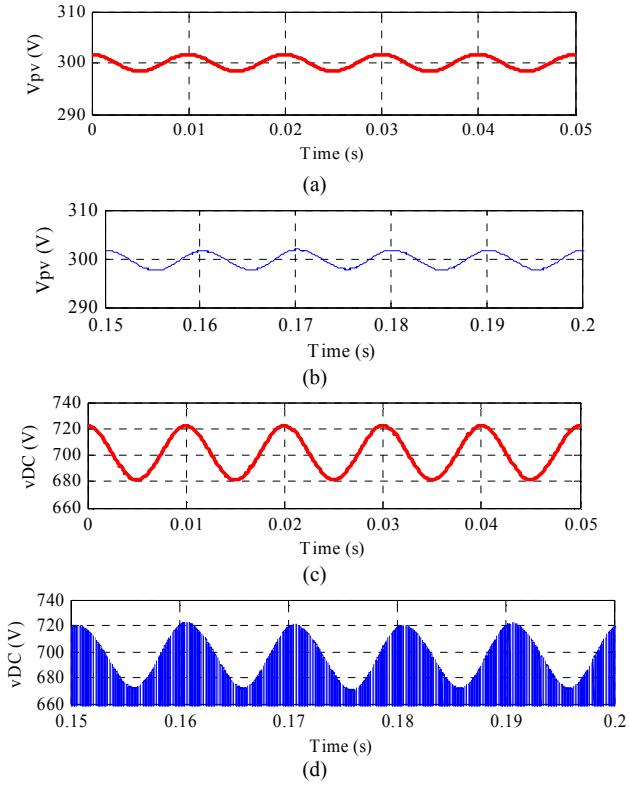

Fig. 9. Calculated and simulated results of PV panel voltage and dc-link voltage in one qZS H-bridge module. (a, b) for PV panel voltage v_{PV} from 2ω–ripple model and simulation, respectively; (c, d) for dc-link peak voltage from 2ω–ripple model and dc-link voltage from simulation, respectively.

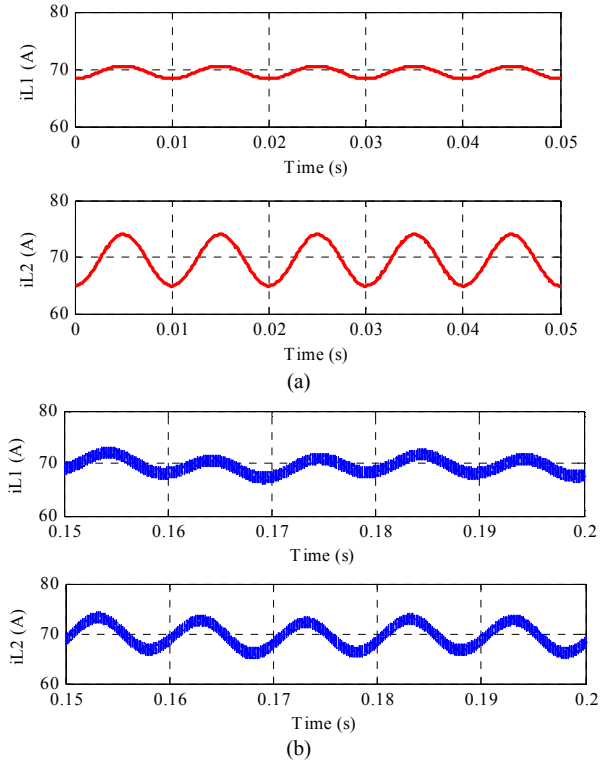

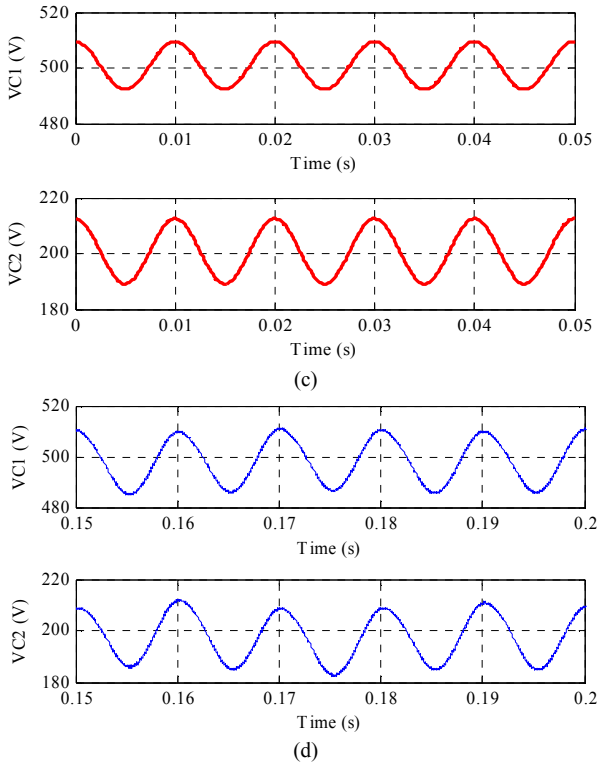

Fig. 10. Calculated and simulated results of inductor currents and capacitor voltages in one qZS H-bridge module. (a) Inductor currents i_{L1} and i_{L2} from 2ω–ripple model; (b) inductor currents i_{L1} and i_{L2} from simulation; (c) capacitor voltages v_{C1} and v_{C2} from 2ω–ripple model and (d) capacitor voltages v_{C1} and v_{C2} from simulation.

VI. Conclusion

In this paper, an effective impedance design method for reducing the 2ω voltage and current ripples in qZS H-bridge PV inverter module of qZS-CMI based MW-scale MV PV power system was proposed. A 2ω-ripple model of qZS network with PV panel terminal capacitance was established. The effects of impedance parameters on 2ω ripples were discussed, which demonstrated that the 2ω ripple of qZS inductor-L_1 current is smaller than that of inductor-L_2 current when considering the PV panel internal resistance; the PV panel terminal capacitance can reduce the 2ω ripples of PV voltage; meanwhile, the qZS capacitance and inductance have combined effects on 2ω ripples of qZS inductor currents. And therewith, impedance design of a 21 kW system was presented to limit those ripples passively. Simulation results verified the deduced ripple model and proposed impedance design, offering an effective design method for the future application of such topology.

Acknowledgment

This paper was made possible by NPRP-EP grant # [X-033-2-007] from the Qatar National Research Fund (a member of Qatar Foundation). The statements made herein are solely the responsibility of the authors.

REFERENCES

[1] T. Kerekes, E. Koutroulis, D. Séra, R. Teodorescu, M. Katsanevakis, "An optimization method for designing large PV plants," *IEEE Journal of Photovoltaics*, vol.3, no.2, pp.814-822, April 2013.

[2] W. Li and X. He, "Review of non-isolated high-step-up dc/dc converters in photovoltaic grid-connected applications," *IEEE Trans. Ind. Electron.*, vol. 58, no. 4, pp. 1239-1250, Apr. 2011.

[3] S. Daher, J. Schmid, and F. Antunes, "Multilevel inverter topologies for stand-alone PV systems," *IEEE Transactions on Industrial Electronics*, vol.55, no.7, pp.2703-2712, July 2008.

[4] B. Ge, *Energy Stored Cascade Multilevel Photovoltaic Grid-Tie Power Generation System*, China Patent CN101917016 A, Dec. 15, 2010.

[5] D. Sun, B. Ge, F.Z. Peng, A. Haitham, D. Bi, Y. liu, " A new grid-connected PV system based on cascaded H-bridge quasi-Z source inverter," in *2012 IEEE International Symposium on Industrial Electronics (ISIE)*, pp.951-956, 28-31 May 2012.

[6] Yan Zhou, Liming Liu, Hui Li, " A high-performance photovoltaic module-integrated converter (MIC) based on cascaded quasi-Z-source inverters (qZSI) using eGaN FETs," *IEEE Transactions on Power Electronics*, vol.28, no.6, pp.2727-2738, June 2013.

[7] Yushan Liu, Baoming Ge, Haitham Abu-Rub, F.Z. Peng, "A Modular Multilevel Space Vector Modulation for Photovoltaic Quasi-Z-Source Cascade Multilevel Inverters", *2013 Twenty-Eighth Annual IEEE Applied Power Electronics Conference and Exposition (APEC)*, vol., no., pp. 714-718, 17-21 March 2013.

[8] Yushan Liu, Baoming Ge, Haitham Abu-Rub, FangZ. Peng, "An Effective Control Method for Quasi-Z-Source Cascade Multilevel Inverter based Grid-tie Single-Phase Photovoltaic Power System", *IEEE Transactions on Industrial Informatics,* vol.10, no.1, pp.399-407, Feb. 2014.

[9] Yaosuo Xue, Baoming Ge, Fang Zheng Peng, "Reliability, efficiency, and cost comparisons of MW-scale photovoltaic inverters," in *2012 IEEE Energy Conversion Congress and Exposition (ECCE)*, 15-20 Sept. 2012, pp.1627-1634.

[10] Yushan Liu, Baoming Ge, Haitham Abu-Rub, FangZ. Peng, "Phase-shifted Pulse-Width-Amplitude Modulation for Quasi-Z-Source Cascade Multilevel Inverter Applied to PV Power Systems", *2013 IEEE Energy Conversion Congress & Exposition* (*ECCE*), Denver, USA, vol., pp. 94-100, 15-20 Sept. 2013.

[11] J. Anderson and F. Z. Peng, "Four quasi-Z-Source inverters," in *PESC '08 - 39th IEEE Annual Power Electronics Specialists Conference, June 15, 2008 - June 19, 2008*, Rhodes, Greece, 2008, pp. 2743-2749.

[12] Y. Li, J. Anderson, F. Z. Peng, and D. L. Liu, "Quasi-Z-Source inverter for photovoltaic power generation systems," *2009 IEEE Applied Power Electronics Conference and Exposition (APEC), Vols 1- 4,* pp. 918-924, 2009.

[13] B. Ge, H. Abu-Rub, F. Peng, Q. Lei, de Almeida A., Ferreira F., D. Sun, Y. Liu, "An energy stored quasi-Z-source inverter for application to photovoltaic power system," *IEEE Trans. Ind. Electron.,* vol.60, no.10, pp.4468-4481, Oct. 2013.

[14] H. Abu-Rub, A. Iqbal, Sk. Moin Ahmed, F. Z. Peng, Y. Li, G. Baoming, "Quasi-Z-Source Inverter-Based Photovoltaic Generation System With Maximum Power Tracking Control Using ANFIS," *IEEE Transactions on Sustainable Energy*, vol.4, no.1, pp.11-20, Jan. 2013.

[15] Yi Huang, Miaosen Shen, F.Z. Peng, Jin Wang, " Z-Source Inverter for Residential Photovoltaic Systems," *IEEE Transactions on Power Electronics*, vol.21, no.6, pp.1776-1782, Nov. 2006.

[16] M. Hanif, M. Basu, K. Gaughan, "Understanding the operation of a Z-source inverter for photovoltaic application with a design example," *IET Power Electronics*, vol.4, no.3, pp.278-287, March 2011.

[17] Yushan Liu, BaomingGe, Haitham Abu-Rub, FangZ. Peng, "Control System Design of Battery-Assisted Quasi-Z-Source-Inverter for Grid-Tie Photovoltaic Power Generation", *IEEE Transactions on Sustainable Energy*, vol.4, no.4, pp.994-1001, Oct. 2013.

[18] S. Rajakaruna and L. Jayawickrama, "Steady-State Analysis and Designing Impedance Network of Z-Source Inverters," *IEEE Transactions on Industrial Electronics,* vol. 57, pp. 2483-2491, July 2010.

[19] Yifan Yu, Qianfan Zhang, Xiaofei Liu, Shumei Cui, "DC-link voltage ripple analysis and impedance network design of single-phase Z-source inverter," *Proceedings of the 2011-14th European Conference on Power Electronics and Applications (EPE 2011)*, vol., no., pp.1-10, Aug. 30-Sept. 1, 2011.

[20] Dongsen Sun, Baoming Ge, Xingyu Yan, Daqiang Bi, Haitham Abu-Rub, Fang Z. Peng, "Impedance Design of Quasi-Z Source Network to Limit Double Fundamental Frequency Voltage and Current Ripples in Single-Phase Quasi-Z Source Inverter", *2013 IEEE Energy Conversion Congress & Exposition* (*ECCE*), Denver, USA, vol., pp. 2745-2750, 15-20 Sept. 2013.